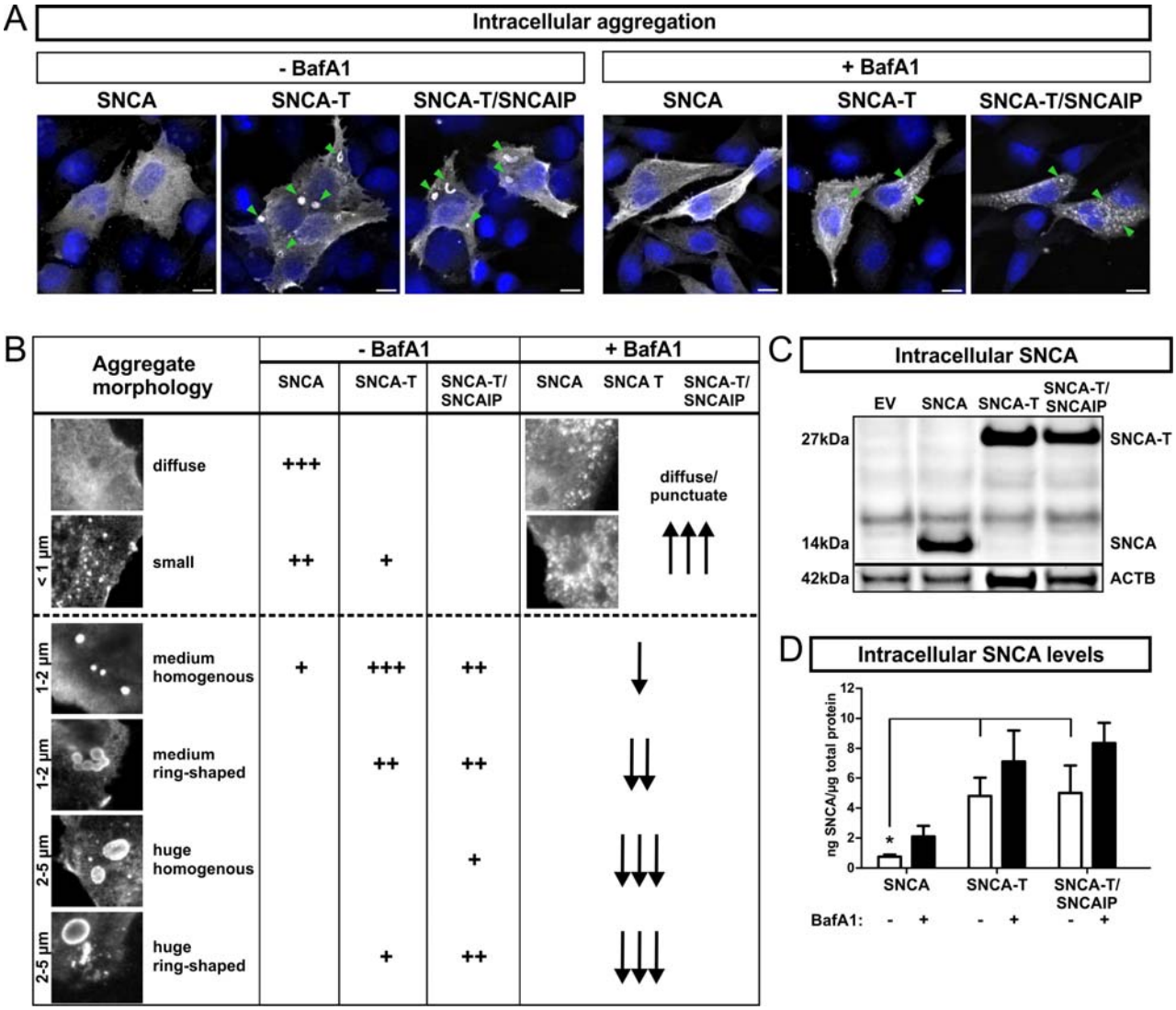

Figure S1. Modulation of aggregate formation by BafA1 in transfected H4 cells. Immunocytochemistry of H4 cells transfected with SNCA, SNCA-T**,** and both SNCA-T and SNCAIP with an antibody against human SNCA. (**A**) H4 cells transfected with SNCA-T and SNCAIP exhibit intracellular aggregates 36 h post-transfection. BafA1 treatment reduces the presence of large intracellular SNCA-T aggregates resulting in smaller accumulations and a punctate SNCA pattern. Green arrowheads indicate intracellular aggregate and accumulation formation. Scale bar = 5 µm. (**B**) Scheme of intracellular SNCA distribution and aggregate formation in H4 cells expressing low-aggregating SNCA and high-aggregating SNCA-T, and both SNCA-T and SNCAIP as revealed by immunocytochemistry. Plus signs indicate the representative frequency of distinct types of aggregates in aggregate-bearing cells chosen for analysis. BafA1 treatment leads to a diffuse and punctuate pattern of SNCA within H4 cells for all constructs.

Scale bar = 5 μm. (**C**) Representative western blots of protein lysates probed for SNCA (14 kDa) and SNCA-T (27 kDa) and ACTB as loading control (42 kDa). (**D**) Western blot quantification of SNCA expression levels in H4 cells transfected with SNCA, SNCA-T, and both SNCA-T and SNCAIP 36 h post-transfection. 25 ng of recombinant human SNCA served as calibrator for SNCA amounts. ALP inhibition by BafA1 slightly increases intracellular SNCA compared to untreated cells. All values are mean + s.e.m.; differences are significant at (*) $P < 0.01$.

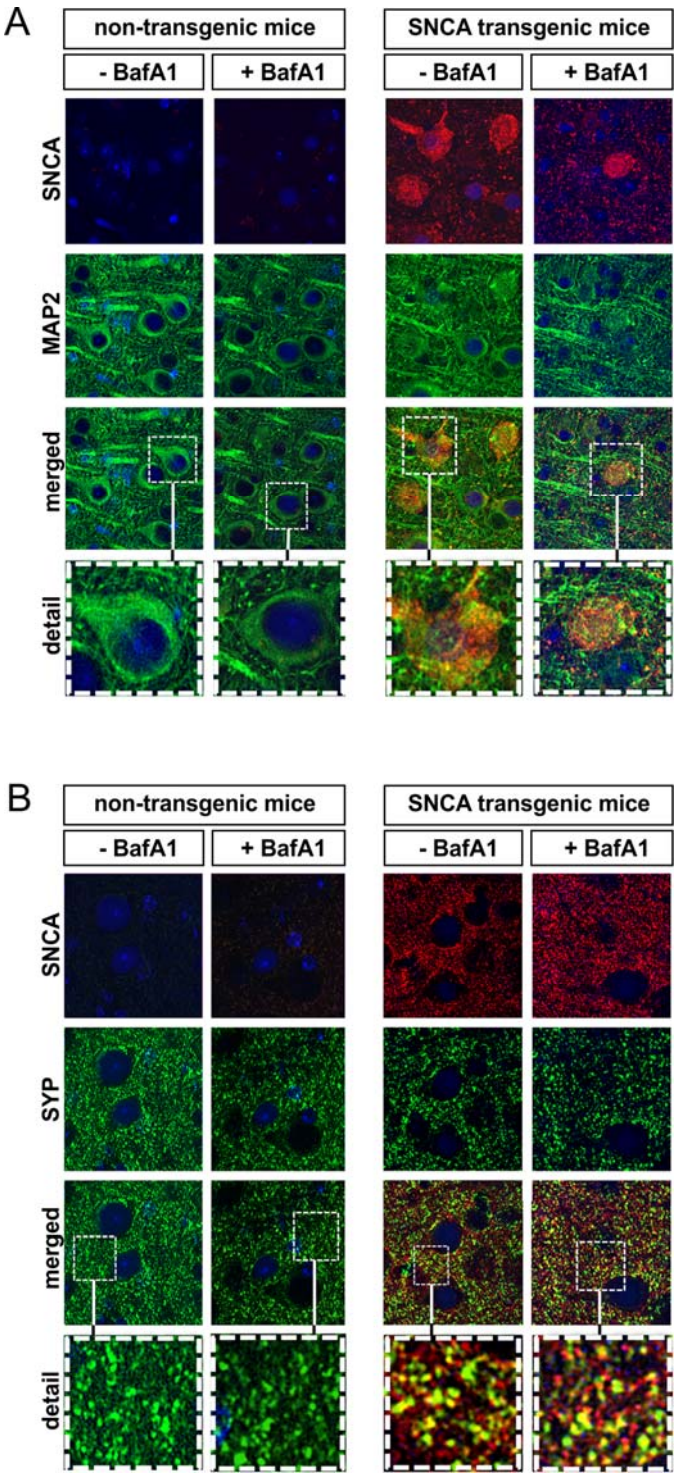

Figure S2. Cellular localization of SNCA in transgenic mice. (**A**) Confocal images of the $MAP2^+$ (green) somatic and dendritic compartment double-labeling for SNCA (red) in the neocortex of SNCA transgenic mice either treated with BafA1 or vehicle. SNCA is expressed in the soma and occasionally in dendrites. (**B**) Confocal images of the SYP^+ (green) axonal and synaptic compartment double-labeling for SNCA

(red) in the neocortex of SNCA transgenic mice either treated with BafA1 or vehicle. BafA1 treatment enhances the punctuate structures in the neuropil.

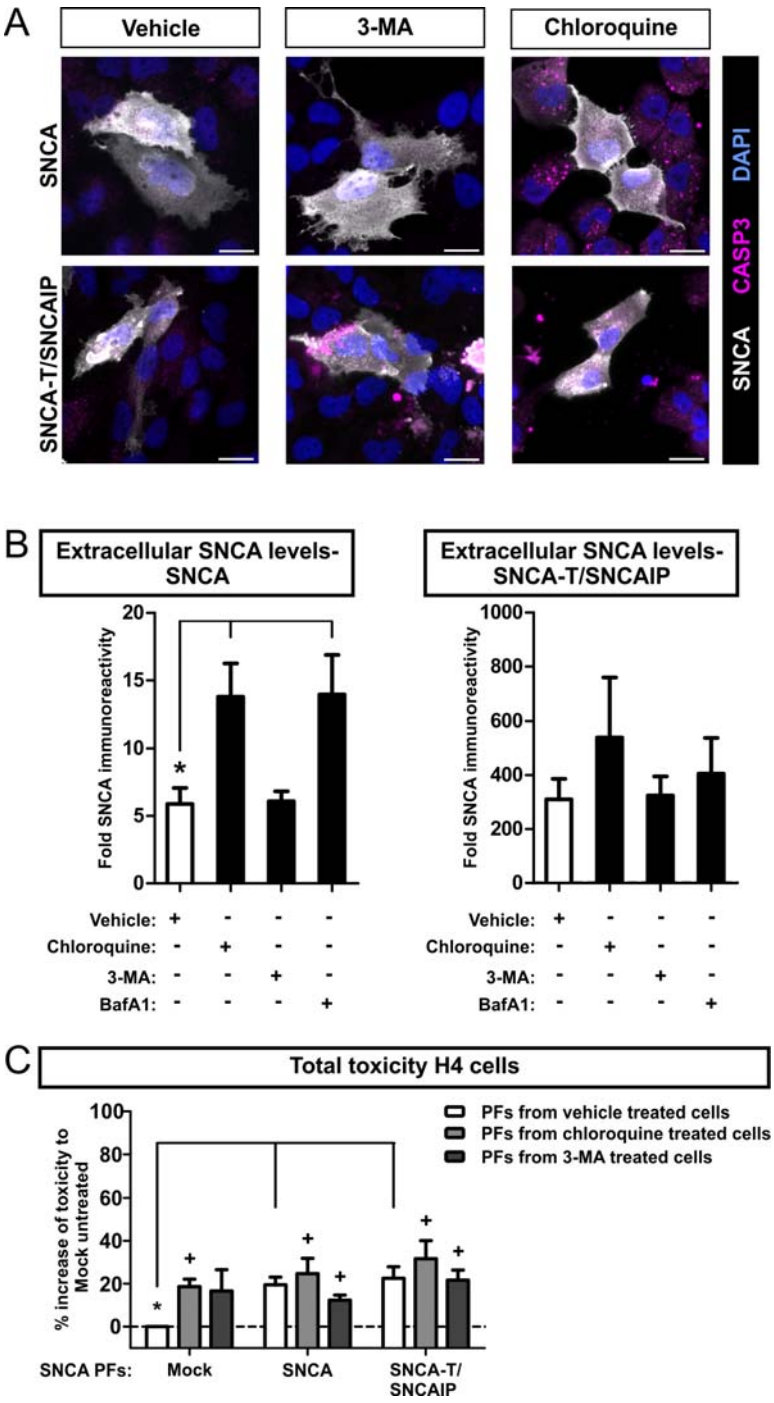

Figure S3. Modulation of SNCA release and toxicity induction by other ALP inhibitors. (**A**) Immunocytochemical staining of SNCA (white) and activated CASP3 (pink) in H4 cells expressing low-aggregating SNCA and high-aggregating SNCA-T and SNCAIP after treatment with either vehicle, 3-methyladenine (3-MA), or chloroquine (CQ). Scale bar = 20 µm. (**B**) Dot blot quantification of extracellular SNCA levels in the medium of H4 cells expressing high-aggregating and SNCA-T low-aggregating SNCA compared to mock-transfected control cells 36 h post transfection. Treatment with 50

μM CQ for 12 h results in increased levels of extracellular SNCA in the medium of H4 cells transfected with SNCA, as well as SNCA-T and SNCAIP compared to untreated cells. (**C**) Exposure of naïve H4 cells to PFs prepared from conditioned medium of untreated, 3-MA, or CQ-treated cells expressing low-aggregating SNCA or high-aggregating SNCA-T and SNCAIP. No SNCA-mediated toxicity induction by 3-MA or CQ can be measured using ToxiLight. All values are mean + s.e.m.; differences are significant at (*) $P< 0.01$ and at (+) $P < 0.05$.

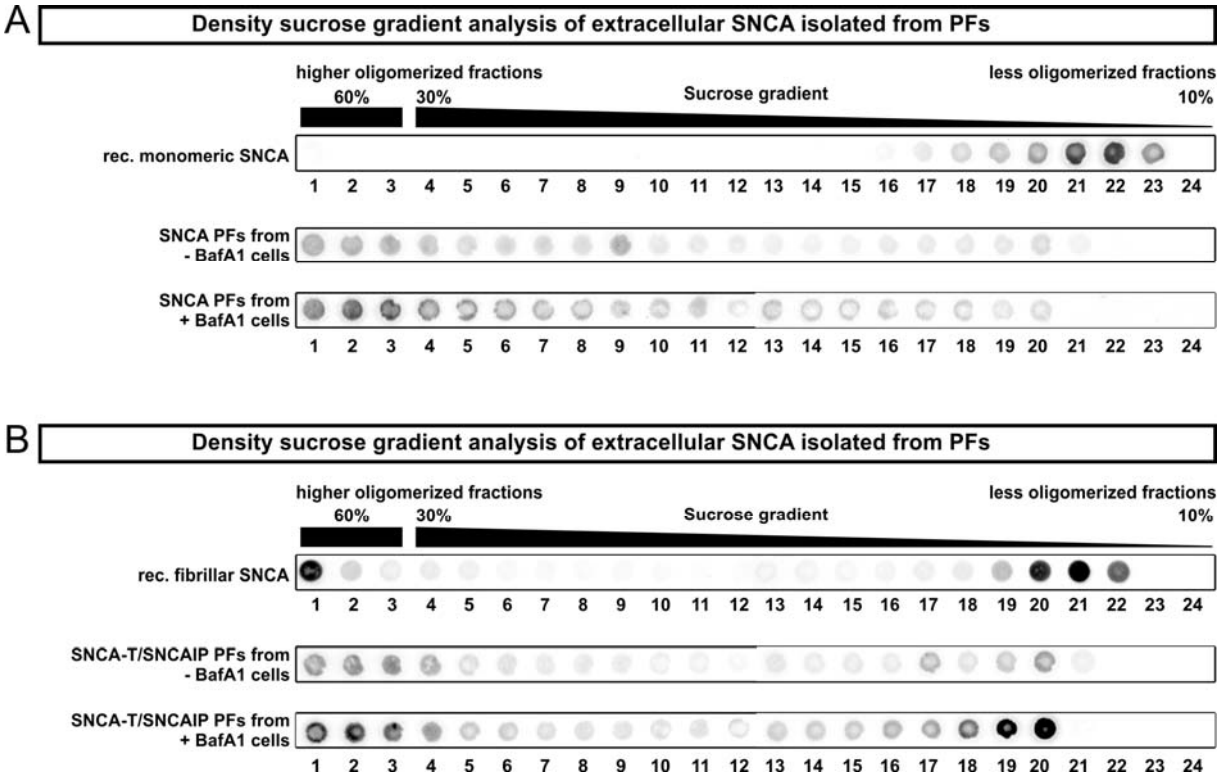

Figure S4. Oligomerization analysis of SNCA associated with particle fractions prepared from CM. Representative Dot blots displaying SNCA immunoreactivity in the different fractions collected after density sucrose gradient centrifugation. Fractions 1 to 3 represent the 60% sucrose cushion containing higher oligomerized SNCA species. Fractions 4 to 24 consist of decreasing percentages of sucrose and represent a decline of oligomerization. Recombinant monomeric and fibrillar SNCA are shown as controls. (**A**) PFs prepared from conditioned medium of BafA1-treated cells overexpressing SNCA display a shift to more oligomerized species that can be detected in fractions 1 to 3. (**B**) PFs prepared from conditioned medium of BafA1-treated cells overexpressing SNCA-T and SNCAIP display a shift to less oligomerized species that can be detected in fractions 18 to 20. Note that monomeric species as seen for recombinant SNCA in fractions 21 to 24 cannot be detected in SNCA associated with PFs.

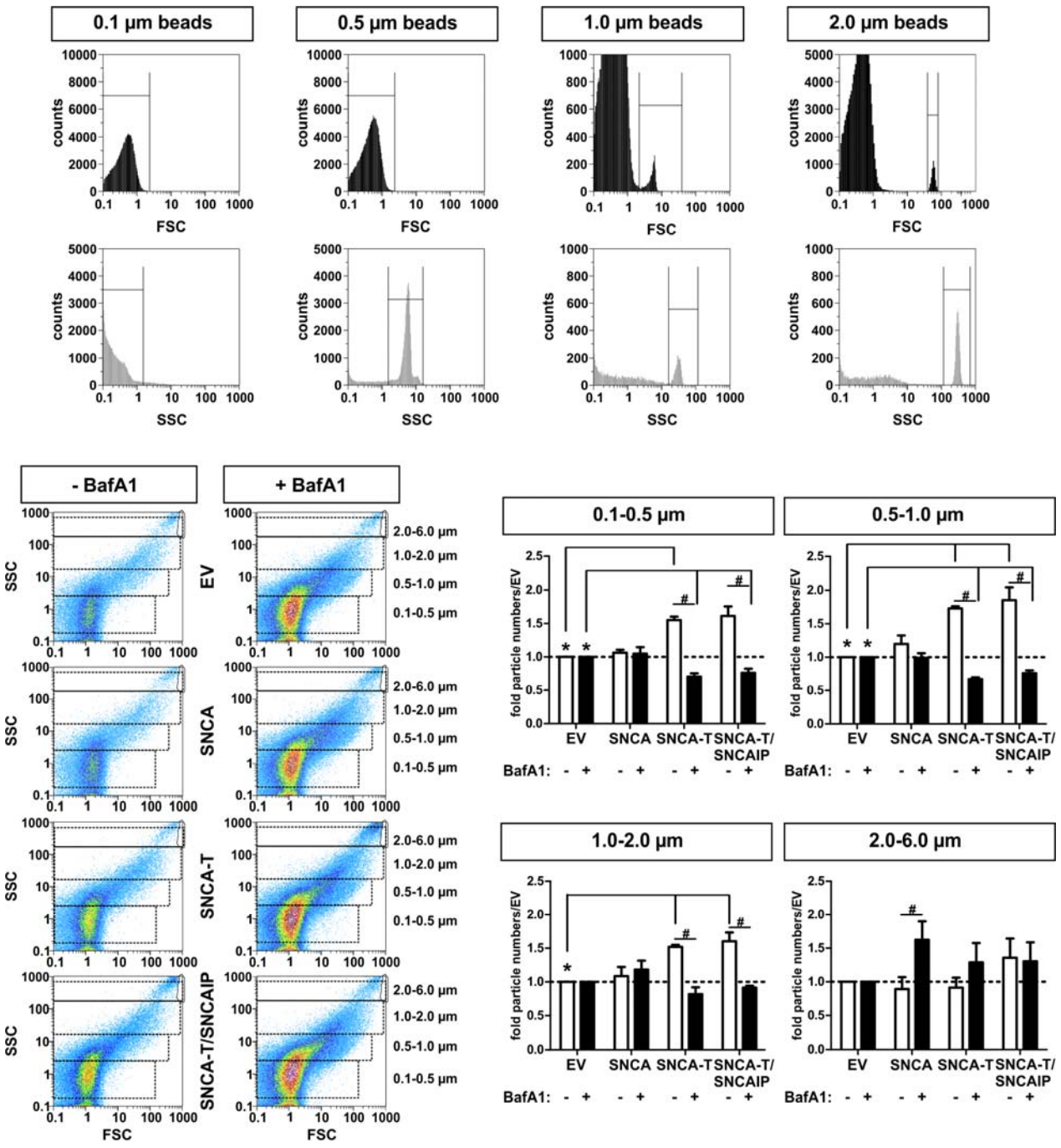

Figure S5. Different sizes of microparticles released from transfected H4 cells. Histograms of synthetic beads of known size (0.1, 0.5, 1.0, 2.0 µm) reflect size (FSC) and granularity (SSC) of microparticles. Representative scatter plots of microparticles resulting from transfected H4 cells after BafA1 treatment compared to untreated cells depict different populations in terms of size and granularity (left). SNCA-T and SNCAIP expression increases the number of released microparticles of different size whereas SNCA

expression has no effect. ALP inhibition by BafA1 attenuates the stimulatory effect of SNCA-T and SNCAIP. All values are mean + s.e.m.; differences are significant at (#) $P < 0.01$ and at (#) $P < 0.05$.